

Dynamical transition between two mesons and a tetraquark.

I. A. Toledano Juárez and G. Toledo Sánchez

Instituto de Física, Universidad Nacional Autónoma de México. México D. F. C.P. 04510

(Dated: September 20, 2016)

We consider a system composed of two identical light quarks (qq) and two identical antiquarks ($\bar{Q}\bar{Q}$) that can be linked either as two mesons or as a tetraquark, incorporating quantum correlations between identical particles and an effective many-body potential between particles. We perform a 3-D Monte Carlo simulation of the system, considering the configurations allowed to form: i) Only two mesons, ii) Only tetraquark and iii) two mesons and tetraquark. We characterize each case and determine whether it is energetically more favorable to form a tetraquark or two mesons, as a function of the interparticle separation distance which, for a fixed number of particles, can be identified as a particle density. We determine how the two mesons, which dominate the low density regime, mixes with a tetraquark state as the density increases. Properties like the mean square radius and the two-particle correlation function are found to reflect such transition, and we provide a parameterization of the diquark correlation function in the isolated case. We track the dynamical flipping among configurations to determine the recombination probability, exhibiting the importance of the tetraquark state. We analyze the four-body potential evolution and show that its linear behavior is preserved, although the slope can reflect the presence of a mixed state. Results are shown for several light-quarks to heavy-antiquarks mass ratios whenever they are found to be relevant.

PACS numbers: 14.40.Rt, 12.38.Lg, 12.39.Pn, 12.39.Jh

I. INTRODUCTION

The formation of multi-quark systems can have important implications in the phenomena we observe in nature, from an enhanced spectroscopy to quark recombination effects. A tetraquark state, the simplest of this kind of systems, has been extensively studied from the theoretical and experimental point of view. Recently, experimental research has provided strong evidence on the formation of such state [1–3]. These findings signal a new era in hadron spectroscopy, where more refined modeling and a better understanding of the strong interaction, in the low energy regime, is required. Since the early years of the quark model, theoretical studies have been performed to inquiry on the existence and stability of the tetraquark as an isolated object [4–16], and how its mixing with a meson state can help us to understand the observed spectroscopy of states like the σ meson [16, 17]. Less attention has been paid to the features of the tetraquark formation as two mesons are forced to approach each other as it could happen in a meson-meson collision or, on the opposite, when the four quarks are produced very close in space as in the WW decay, which eventually freeze out to two mesons [18, 19]. At which stage they turn into a tetraquark or mixed state? and how their properties reflect such modification? are certainly important questions.

In the present work we address these questions using an effective model (String-Flip Model) to mimic the strong interaction among quarks. For definiteness we consider two identical light quarks qq (denoted by u) and two identical antiquarks $\bar{Q}\bar{Q}$ (denoted by d, s, c and b , depending on the mass ratio respect to the light one). The seminal work by Lenz *et al.* [7] laid down a procedure to describe such a system in this context and found its gen-

eral properties, as isolated objects, using a harmonic potential interaction. Here, we perform a 3-D Monte Carlo simulation of the system including quantum correlations between particles to determine whether it is energetically more favorable to form a 4-body state (tetraquark) or two mesons, as a function of the interparticle separation which, for a fixed number of particles, can be identified as a particle density. We are interested in s-wave states where tensor and spin interaction effects are expected to be negligible in the gross features of the properties. In section II, we set the basis to identify a quark-antiquark state interacting via a linear potential and elaborate on a variational approach. In section III, we describe the dynamical quark recombination model and generalize the variational two-body wavefunction to a four-body system. In section IV, we describe the energy evaluation from Monte Carlo simulation. In section V, we show the results on: A) The determination of the optimal variational parameter and system energy, B) The hadron radial distribution characterization, C) The two-particle correlation functions, among the two mesons and among quarks. In particular we provide a parameterization of the diquark correlation function and the static structure factor, D) The dynamical recombination probabilities among mesons with/without tetraquark configurations, E) We characterize the four body potential, estimating its linear behavior and its strength as an effective contact interaction. The conclusions are presented in section VI.

II. QUARK-ANTIQUARK STATE WITH LINEAR POTENTIAL

Let us start with the description of the exact solution and the variational approach of a meson state, composed

of a quark and an antiquark of mass m_1 and m_2 respectively. The strong interaction between this pair can be represented by a flux tube [6], which can be effectively described by a linear potential $V[\vec{r}_1, \vec{r}_2] = k|\vec{r}_1 - \vec{r}_2| = kr$ where k is an interaction constant and $r = |\vec{r}_1 - \vec{r}_2|$ is the relative distance between them. Lattice QCD studies have confirmed the linear behavior of the interaction among quarks at large distances [20].

A. Exact solution

For a three-dimensional space, one can analytically solve the corresponding Schrödinger equation:

$$\left[\frac{P_1^2}{2m_1} + \frac{P_2^2}{2m_2} + kr \right] \Psi(\vec{r}_1, \vec{r}_2) = E \Psi(\vec{r}_1, \vec{r}_2). \quad (1)$$

Since the potential depends only on the relative distance, we can use the center of mass (\vec{R}) and relative distance (\vec{r}) vectors:

$$\vec{R} \equiv \frac{m_1 \vec{r}_1 + m_2 \vec{r}_2}{m_1 + m_2}; \quad \vec{r} \equiv \vec{r}_1 - \vec{r}_2, \quad (2)$$

and the wave function can be set as:

$$\Psi(\vec{R}, \vec{r}) = \Phi(\vec{R})\rho(\vec{r}). \quad (3)$$

We can neglect the center of mass contribution and focus in the relative distance Schrödinger equation. Considering a spherical symmetry ($l=0$), the radial solution can be set as $U(r) = r\rho(r)$, such that the radial equation becomes:

$$-\frac{1}{2\mu} \frac{d^2 U(r)}{dr^2} + krU(r) = EU(r), \quad (4)$$

where $\mu \equiv m_1 m_2 / (m_1 + m_2)$ is the reduced mass. Switching to the variable

$$\xi \equiv \left(r - \frac{E}{k} \right) (2\mu k)^{1/3}; \quad \eta(\xi) = U(r) \quad (5)$$

The Schroedinger Eqn. (4) takes the following form:

$$\frac{d^2}{d\xi^2} \eta(\xi) - \xi \eta(\xi) = 0, \quad (6)$$

whose general solution is a linear combination of the Airy functions $\text{Ai}(\xi)$ and $\text{Bi}(\xi)$. The second function is not considered as it has a bad behavior at large distances ($\xi \rightarrow \infty$, $\lim \text{Ai}(\xi) = 0$ and $\lim \text{Bi}(\xi) = \infty$). Thus, the solution is:

$$\eta(\xi) = \text{Ai}(\xi) \quad (7)$$

The boundary condition at the origin $U(0) = 0$ requires

$$\eta\left(-\frac{E}{k} (2\mu k)^{1/3}\right) = 0, \quad (8)$$

corresponding to the zeros of the Airy function ξ_n , which then define the eigen-energies E_n :

$$E_n = \left[\frac{k^2}{2\mu} \right]^{1/3} |\xi_n| \quad (9)$$

and eigen-functions:

$$\rho_n(r) = \frac{1}{r} \text{Ai}\left(r [2\mu k]^{1/3} - \xi_n\right). \quad (10)$$

The ground state corresponds to the first zero of the Airy function, with energy $E_0 = 2.3381$, in $m_1 = m_2 = m = k = 1$ units.

B. Meson variational wave function

Previous studies have explored how to approach a variational wave function that can account for the meson energy [8–10, 21]. Here, we describe, in similar fashion, a family of 3-D variational wave functions that approach this value and find analytical expressions for the expected variational parameter, energy and mean square radius. The general variational wave function takes the following form:

$$F_{\lambda,b}(r) = A e^{-\lambda r^b}, \quad (11)$$

where A is a normalization term, b and λ are variational parameters and r is the relative coordinate of the two-body system. We have found that using $b = 1.74716$ and $\lambda = 0.350132$, the wave function reproduces the exact minimum energy value within a 1% error. Based on this analysis, we fix the variational parameter $b = 3/2$ and leave the λ parameter as the only free parameter. Then, the normalized meson variational wave function becomes:

$$F_\lambda(r) = \sqrt{\frac{3\lambda^2}{2\pi}} e^{-\lambda r^{3/2}}. \quad (12)$$

Analytical results can be obtained for the properties of the meson for this form of the variational wave function. The value of λ minimizing the energy is:

$$\lambda_0 = \frac{2\sqrt{k\mu}}{3}, \quad (13)$$

corresponding to an energy of

$$E_0 = \frac{3^{5/3} k \Gamma\left(\frac{8}{3}\right)}{2^{7/3} (k\mu)^{1/3}}, \quad (14)$$

which is only around 3% higher than the exact solution (see Table I). The mean square radius for the meson can be obtained following the general definition:

$$\langle r_M^2 \rangle \equiv \left\langle \sum_{i=1}^2 (\vec{r}_i - \vec{R})^2 \right\rangle \quad (15)$$

m_2/m_1	λ_0	E_0	E_{exact}	$\langle r_M^2 \rangle_0$
1	0.4714	2.3472	2.33811	1.50255
1.44643	0.5125	2.2197	2.21106	1.38885
4.6131	0.6043	1.9889	1.98118	1.52605
14.0774	0.6441	1.9061	1.8987	1.73656

TABLE I: Optimal variational parameter and energy, the exact energy and mean square radius for different mass ratios respect to the lightest u mass, m_1 .

In the meson case with particles of mass m_1 and m_2 , it becomes

$$\langle r_M^2 \rangle_0 = \frac{m_1^2 + m_2^2}{(m_1 + m_2)^2} \frac{3^{4/3}}{4} \Gamma\left(\frac{10}{3}\right),$$

where the subindex $_0$ is used everywhere to denote the isolated case. We can extend this analysis for quarks of different masses, in particular considering the constituent masses of the d, s, c and b quarks, we set the ratio of their masses respect to the u quark mass, taken as reference [22]. In Table I, we show the corresponding optimal variational parameter (λ_0), the variational energy (E_0), the exact energy (E_{exact}) and the variational radius ($\langle r_M^2 \rangle_0$) for the different mass ratios. We denote u mass as m_1 , and m_2 corresponds to effective d, s, c and b masses. These results will be used as reference when extending to a four-body system.

III. FOUR-BODY SYSTEM

Using the previous results, we can now extend our study to a four-body system composed of two identical u -like quarks (qq) and two identical antiquarks ($\bar{Q}\bar{Q}$), which can be d, s, c and b -like. To simplify the notation, we will refer to this four-body system by qQ . At very low density, where the distance between quarks is large, the model must reproduce a system of two isolated mesons. In addition, as the density increases, the interparticle separation becomes small allowing the interaction between the two mesons, which can be represented by quark exchange or a truly four-body interaction. All over, the Pauli blocking among identical particles must be enforced, allowing the system to behave like a free Fermi system at very high densities. Here, we rely on the String-Flip Model [7, 23, 24] which has been also used to study dense matter systems [25, 26], to describe the dynamical transition among these regimes.

A. String-flip Potential

To model such a system, we need to capture the properties of the strong interaction. In particular, the strong interaction of a many-body system can be well

approached by considering that the quarks are connected by gluon flux tubes [6] according to a configuration producing the lowest energy state of the whole system.

Let us denote the position of the particles by \vec{r}_1 and \vec{r}_2 and the antiparticles by \vec{r}_3 and \vec{r}_4 . The way to link the four particles of the system consistent with the QCD restrictions of color neutrality is two-fold:

i) The system is composed of two mesons. Then, using the linear potential per pairs $V(\vec{r}_i, \vec{r}_j) \equiv k|\vec{r}_i - \vec{r}_j| = kr_{ij}$, the total potential can be either

$$V_{m1} = V(\vec{r}_1, \vec{r}_3) + V(\vec{r}_2, \vec{r}_4) \quad (16)$$

or

$$V_{m2} = V(\vec{r}_1, \vec{r}_4) + V(\vec{r}_2, \vec{r}_3). \quad (17)$$

ii) The system is composed of a tetraquark. In this case, the shortest path linking the four particles is given by the Steiner-tree, which uses two auxiliary vectors (denoted by \vec{k} and \vec{l}) to minimize the length of the configuration. The vector \vec{k} links the diquark sub-system and the vector \vec{l} the anti-diquark one. The diquark and anti-diquark are considered to belong to the $\mathbf{3}$ and $\bar{\mathbf{3}}$ representations of the color SU(3) symmetry, respectively. Thus, the total system form a color singlet state. The interaction among particles in such representations is attractive with a strength a half of the quark-antiquark interaction. Since there is no direct link between particles but rather an interaction via auxiliary vectors, we use such strength as the same among all of them. This form of the potential has been shown to be consistent with the flux tube picture [6] and found, in the Lattice QCD framework, to follow a linear behavior at large distances [27]. Thus, the potential becomes:

$$V_{4Q} = \sum_{i=1}^2 V(\vec{k}, \vec{r}_i)/2 + \sum_{j=3}^4 V(\vec{l}, \vec{r}_j)/2 + V(\vec{k}, \vec{l})/2, \quad (18)$$

where the $1/2$ factor accounts for the decreasing in the coupling strength. When all these configurations are allowed, the potential of the system is chosen as the one producing the minimum potential energy in a given configuration:

$$V = \min(V_{m1}, V_{m2}, V_{4Q}). \quad (19)$$

B. Variational Wave function

Generalizing the meson result to include all the possible configurations at different densities, we propose the following variational wave function, which reproduces the two isolated mesons at very low densities, allows four-body correlations and incorporates the Fermi correlations as the density increases:

$$\Psi_\lambda = \Phi_{FG}(e^{-\lambda Q}), \quad (20)$$

where λ is the single variational parameter, Q is a function driven by the many-body potential, and Φ_{FG} is the free Fermi system wave function given by a product of Slater determinants, one for each color-flavor combination of quarks. For a four-body system, the Q function takes the following form, depending on the optimal potential at the given configuration, denoted by the sub-index:

$$Q_{m_1} = r_{13}^{3/2} + r_{24}^{3/2}, \quad (21)$$

$$Q_{m_2} = r_{14}^{3/2} + r_{23}^{3/2} \quad (22)$$

or

$$Q_{4Q} = r_{1k}^{3/2} + r_{2k}^{3/2} + r_{kl}^{3/2} + r_{3l}^{3/2} + r_{4l}^{3/2}, \quad (23)$$

where the $3/2$ power is the resemblance of the exact solution of single pairs linked by a linear potential.

The Slater determinants are composed of single wave functions of a particle in a cubic box of side L with Eigen-energy

$$E_n = \frac{\pi^2 \hbar^2}{2mL^2} (n_x^2 + n_y^2 + n_z^2) \quad (24)$$

where $n_x, n_y, n_z = 1, 2, \dots$. We expect this form of the variational wave function to be able to describe the departure from the two-mesons case into the four-body case, while including the identical particles correlations.

We can define a particle density parameter as a measure of the interparticle separation by: $\rho = N/V = 4/L^3$, where N is the number of particles of the system and V is the box volume. For a fixed number of particles, the change in the particle density corresponds to modify the box size and correspondingly to the inter-particle separation.

IV. ENERGY DETERMINATION

The Hamiltonian of 4 particles of momentum \vec{P}_i and mass m_i interacting through the potential V is:

$$H = \sum_{i=1}^4 \frac{\vec{P}_i^2}{2m_i} + V. \quad (25)$$

Using the above variational wave function, the expectation value of each term in the kinetic energy can be set as:

$$\frac{-1}{2m_i Z(\lambda)} \int \Psi_\lambda \partial_i^2 \Psi_\lambda dx \quad (26)$$

where $Z(\lambda) \equiv \langle \Psi_\lambda | \Psi_\lambda \rangle$. Defining $\Psi_\lambda \equiv F_\lambda \Phi$, with $F_\lambda \equiv e^{-\lambda Q}$, then

$$\partial_i^2 \Psi_\lambda = F_\lambda \partial_i^2 \Phi_{FG} + \partial_i^2 F_\lambda \Phi_{FG} + 2\partial_i F_\lambda \partial_i \Phi_{FG}. \quad (27)$$

The first term leads to the noninteracting particle kinetic contribution (T_{FG}) and the remaining terms, after integrating by parts, to:

$$\frac{1}{2m_i Z(\lambda)} \int \Psi_\lambda^2 [\partial_i \ln F_\lambda]^2 dx. \quad (28)$$

Thus, using the exponential structure of F_λ , this term corresponds to the expectation value of the following function:

$$W_i \equiv \frac{\lambda^2}{2m_i} [\partial_i Q]^2, \quad W \equiv \sum_i^4 W_i, \quad (29)$$

where the sum runs over the coordinates of the four particles. This term can be seen as the correction to the kinetic energy due to the interaction. Thus, the expectation value of the Hamiltonian becomes [25]:

$$\langle H \rangle_\lambda = T_{FG} + \langle W \rangle_\lambda + \langle V \rangle_\lambda. \quad (30)$$

This structure is useful to find the variational parameter λ that minimizes it:

$$\frac{\partial \langle H \rangle_\lambda}{\partial \lambda} = 0. \quad (31)$$

The free kinetic part is given by the sum of the energies of the particles in the box as given by Eqn. (24) and is independent of λ . In order to evaluate $\langle W \rangle$, we need to know the particles coordinates dependence of Q . For the meson configuration, Q is explicitly defined in terms of them, while for the tetraquark it involves the vectors \vec{k} and \vec{l} , whose dependence on the coordinates are not analytically known, in this case numerical determination is used (see Appendix).

V. RESULTS

The expectation values of W and V involves the integration over 12 variables and can be computed using Monte Carlo techniques which, by relying in the importance sampling, turns the integrals into an evaluation of the average of the values of the observable, in particular we use a Metropolis algorithm for the sampling, driven by the square of the wave function. We computed the properties of three systems. The results we present are organized as follows:

- *Two mesons*. In this case, only meson configurations are allowed in the potential. We characterize the meson properties, comparing the results with the expected from the analytical solution in the isolated limit and the departure from them as density increases.
- *Tetraquark*. In this case, only tetraquark configurations are allowed in the potential. We characterize the tetraquark properties in the isolated limit and the departure from them as density increases.

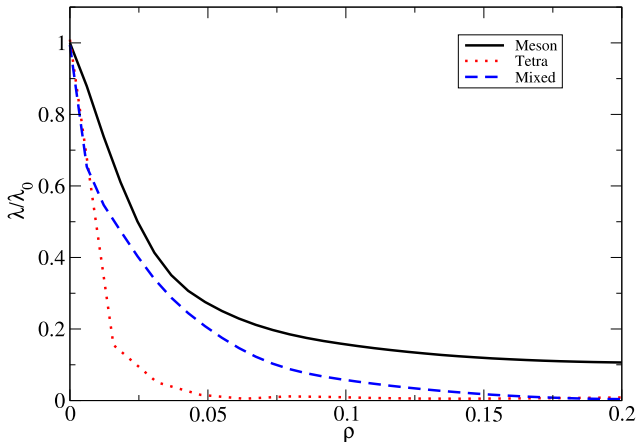


FIG. 1: Variational parameter of the two mesons, tetraquark and mixed systems as a function of the density, for a $ud \equiv uud\bar{d}$ mass assignment. They are normalized to the exact solution in the isolated meson case λ_0 .

- *Mixed*. In this case, all the possible configurations are allowed in the potential. We characterize the meson and tetraquark properties and their modifications due to the presence of the other configuration.

For all the above cases we explored the mass effect by considering the two quarks to be light (u) and the anti-quarks having variable mass to resemble the $m_{d,s,c,b}/m_u$ ratios. Results are presented for several light-quarks to heavy-anti-quarks mass ratios whenever they are found to be relevant.

A. Variational parameter and energy

In order to know the best approach of the variational wave function to the exact solution, we find the optimal value of the variational parameter that minimizes the total energy at a given density. We repeat the procedure for a set of values of the density to know the corresponding evolution of the variational parameter.

In Figure 1, we show the optimal values of the variational parameter of the two mesons, tetraquark and mixed systems as a function of the density, for a $ud \equiv uud\bar{d}$ mass assignment. The behavior for a light-heavy system (ub) is very similar (not shown) thus, for the sake of clarity, we only exhibit this case. The results are normalized to the exact solution in the isolated meson case λ_0 . We observe that they exhibit a smooth evolution from their asymptotic value at low density decreasing to nearly zero at high energy densities, signaling the diminishing effect of the interaction.

In Figure 2, we have plotted the energy of the system (E_4), normalized to the exact solution in the iso-

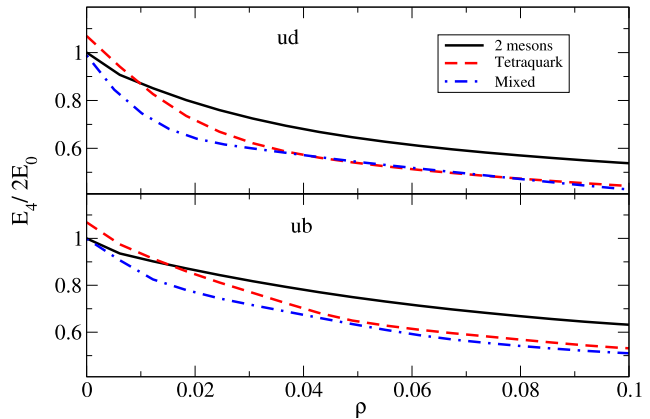


FIG. 2: Energy of the two mesons, tetraquark and mixed systems as a function of the density, normalized to the exact solution of two isolated mesons, $2E_0$. The upper (lower) panel corresponds to a ud (ub) system.

lated meson case ($2E_0$) for the three cases: two mesons, tetraquark and mixed systems, as a function of the particle density. The upper (lower) panel corresponds to a ud (ub) system. We observe that at low density we reproduce the exact result for the two mesons system and the tetraquark system energy is higher. As the density increases, this breach closes and eventually is inverted, signaling that the tetraquark state is more likely at high density. The mixed system turns out to be the one with the lowest energy as it takes advantage of both possible configurations.

B. Radial distribution

Once the optimal variational wave function and energy were characterized, we proceed to compute a set of observables. In particular, the mean square radius (MSR) evolution was obtained, using the optimal pairing information. The mean square radius for the meson or the tetraquark can be obtained following the general definition, Eqn. (15), where the sum runs over the corresponding number of particles. In Figures 3 and 4, we show the density evolution of the MSR for mesons and tetraquarks respectively, normalized to the corresponding value in the isolated case.

The meson MSR evolution is found to be mass ratio dependent. In fact, the light-light combination (ud) decreases faster than the light-heavy case (ub), while the dependence on being in presence of possible tetraquark configurations is mild (solid vs. dashed line) in both cases.

The tetraquark MSR evolution exhibits a mass ratio dependence. The light-light system (solid line) increases

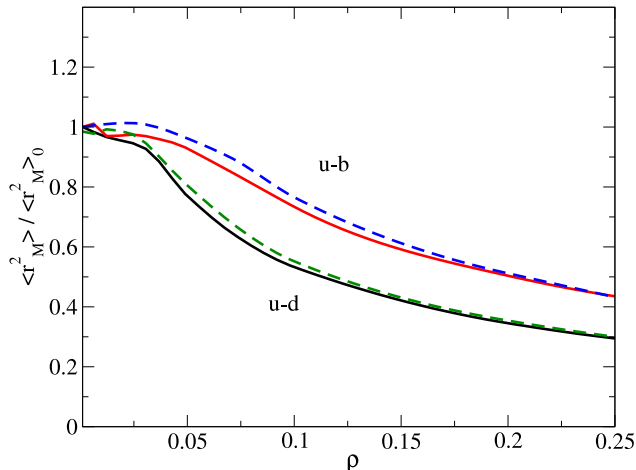


FIG. 3: Meson mean square radius as a function of density, normalized to the isolated case, for light-light (ud) and light-heavy (ub) mass ratios. The solid and dashed line correspond to the meson and mixed system respectively.

m_2/m_1	$2E_0$	E_{4Q_0}	$\langle r_{4Q}^2 \rangle_0$
1	4.6944	5.02 ± 0.02	13.9 ± 0.1
1.44643	4.4394	4.77 ± 0.02	13.2 ± 0.2
4.6131	3.9778	4.24 ± 0.02	12.5 ± 0.3
14.0774	3.8122	4.07 ± 0.02	13.1 ± 0.2

TABLE II: Two mesons energy, Tetraquark energy and mean square radius for different mass ratios respect to the lightest u mass, m_1 in the zero density limit.

in the low density regime and then rapidly decreases. The light-heavy system (dashed line) remains almost unchanged for a relatively large density region and slowly decreases. For both cases we show the modification when considering the presence of the mesons (mixed). Both become large at low density and rapidly decrease as the density increases, approaching the pure tetraquark result. It is very interesting to find out that during the increase of the density, the radial distribution suffers not only contractions but also expansions, which are a result of a competition between the reduction of the interparticle separation and the decrease of the confining potential effect, as it is multiplied by the density decreasing variational parameter.

In Table II, we show the tetraquark energy (E_{4Q_0}) and MSR ($\langle r_{4Q}^2 \rangle_0$) in the limit of zero density, for the different mass ratios. Twice the meson energy ($2E_0$) is also exhibit as reference.

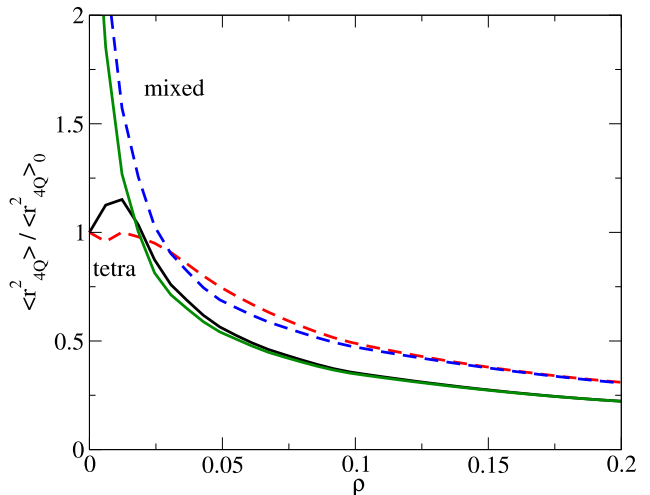


FIG. 4: Tetraquark mean square radius as a function of density, normalized to the isolated case. The solid (dashed) line corresponds to a ud (ub) mass ratios, for the Tetraquark and mixed systems.

C. Correlation functions

Another very useful observable to characterize the properties of the system is the two-particle correlation function [28]. It measures the probability of finding two particles at a relative distance r from each other:

$$g(r) \equiv \frac{V}{4\pi r^2 N^2} \left\langle \sum_{i < j=1}^N \delta(\vec{r} - \vec{r}_{ij}) \right\rangle \quad (32)$$

In Figures 5 and 6 we show the meson-meson correlation function at several densities for the two-mesons and mixed case, respectively. We exhibit the results corresponding to a light-light (ud) system but a similar behavior is observed in the other mass ratio combinations. The comparison between both Figures shows that there is a modification in the meson-meson correlation function by the presence of the tetraquark state at intermediate densities, a bump develops in the near tail of the correlation function, driven by the diquark formation (see below), and fades out as the density increases and all the quark correlations vanish. This may be an alternative observable to have indirect evidence of the tetraquark formation. Note that at low density the separation between the two mesons approaches the result obtained by Lenz et al [7] of $4.66 r/r_M$.

For the two meson case, the quark-quark correlation function at low density is similar to the meson-meson correlation function (not plotted) as the relevant separation distance is driven by the separation between mesons, each one containing a quark.

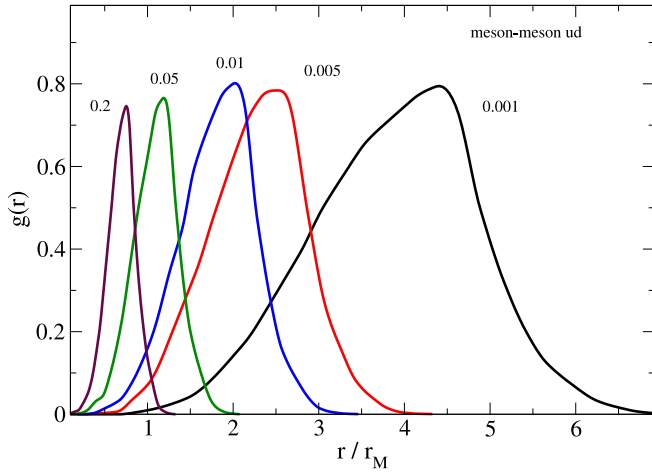


FIG. 5: Meson-meson correlation function at several densities (inner labels). Corresponding to a light-light (ud) system, for the two mesons case.

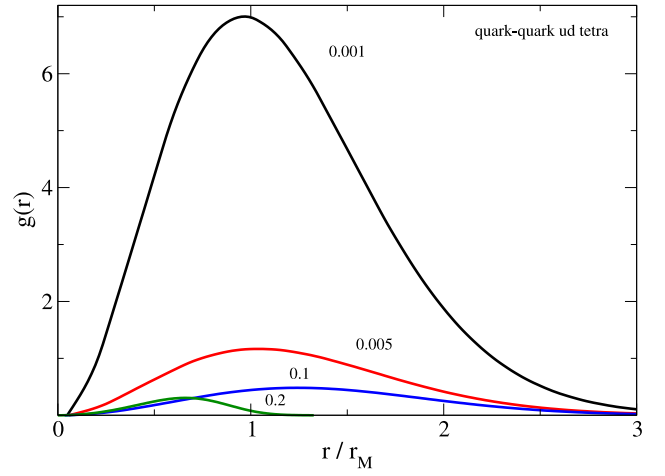


FIG. 7: Quark-quark correlation function at several densities (inner labels), for a light-light (ud) system in the tetraquark case.

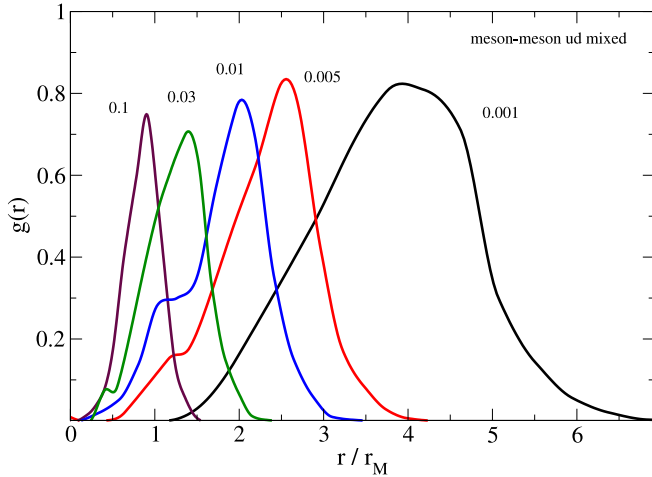


FIG. 6: Meson-meson correlation function at several densities (inner labels). Corresponding to a light-light (ud) system, for the mixed case.

In Figure 7, we show the quark-quark correlation function at several densities (inner labels) for a light-light (ud) system, when only tetraquark configurations are allowed. The diquark formation at low densities is exhibited and, as the density increases, the correlation drops signaling that, although the tetraquark configuration can be identified, the quarks are no longer correlated. Note that the diquark size is similar to the bump observed in the meson-meson correlation function (Figure 6) when tetraquarks are also formed. At low densities the fraction of tetraquarks formed respect to the two mesons is small

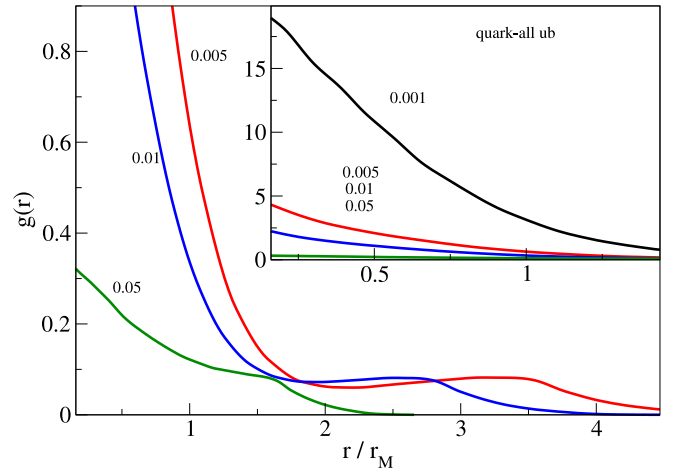


FIG. 8: Correlation between a quark and all the particles regardless of the quantum numbers. Two mesons system.

and has no major effect, it is only in the intermediate density region where this feature becomes relevant.

In Figures 8 and 9, we show the correlation between a quark and all the particles regardless of the quantum numbers, for two mesons and tetraquark systems respectively. Here, we exhibit the case of the light-heavy (ub) combination. Although the general features are similar for other combinations the specific parameters are not. This will be exemplified below, when discussing the zero density limit.

In the zero density limit, the normalized tetraquark

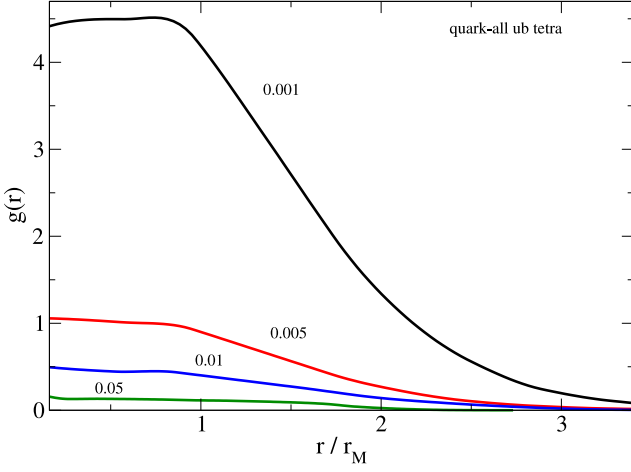


FIG. 9: Correlation between a quark and all the particles regardless of the quantum numbers. Tetraquark system.

System	A_0	A_1	A_2
Quark-quark			
ud	0.64	1.24	1.51
ub	1.13	1.1	1.47
Quark-all			
ud	0.24	1.00	4.60
ub	0.31	0.98	3.19

TABLE III: Diquark and quark-all correlation functions parameters for ud and ub -like mass ratios.

system correlation function for the diquark (quar-quark) and tetraquark (quark-all) can be parameterized by:

$$g(r)_{q-q} = A_0 r^2 e^{-r^{A_2}/A_1^2} \quad (33)$$

and

$$g(r)_{q-all} = A_0 (1 + r/A_1) e^{-r^2/A_2} \quad (34)$$

In Table III, we show the value of the parameters of the diquark and quark-all correlation functions for the light-light and light-heavy cases. Note that the dependence on r of the diquark correlation function is close to others suggested in the literature [29, 30] but in our case it is dynamically obtained. The short distance region shows the competition between the Pauli blocking among the identical particles and the attractive potential.

The static structure factor $S(\mathbf{q})$ can be obtained as the Fourier transform of the correlation function $g(\mathbf{r})$. That is

$$S(\mathbf{q}) = 1 + \frac{N}{V} \int d^3r g(\mathbf{r}) e^{-i\mathbf{q}\cdot\mathbf{r}}. \quad (35)$$

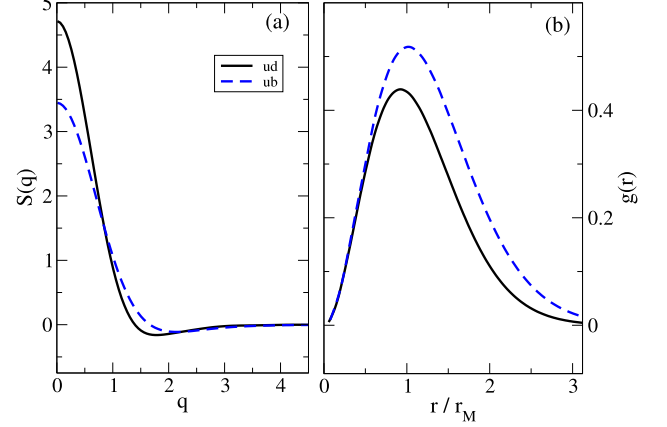


FIG. 10: Diquark static structure factor $S(q)$ (a) and correlation function (b) in the zero density limit, for ud (solid line) and ub (dashed line) tetraquark systems.

In our case we consider the correlation to depend on the magnitude of \mathbf{r} . In Figure 10, we display the diquark static structure factor $S(q)$ (a) and correlation function (b) in the limit of zero density for both ud (solid line) and ub (dashed line) tetraquark systems.

D. Dynamical recombination

The four quark recombination can have important effects in systems where they are produced very close in space. An example can be found in the $WW \rightarrow qq\bar{Q}\bar{Q}$ decay, whose spatial separation at LEP2 energies is around 0.1 fm [18]. Although in the perturbative regime the recombination is small, in the non-perturbative regime the effect may be important. The typical scenarios to estimate the recombination are: Considering spherical or elongated bags color sources and the reconnection is proportional to the overlap of two color sources; strings considered as vortex lines where reconnection takes place when the core of the two string pieces cross each other [19]. The recombination between the two mesons configurations is usually implemented [18, 19]. In our case, we would have, in addition, recombinations similar to tetraquark states which eventually freeze out to two mesons. Here, we characterize the modification to the two mesons recombination induced by the presence of the tetraquark state.

The model requires that the formed clusters must be colorless. The flipping from one configuration to another, driven by the minimal potential energy restriction, is a measure of the dynamical recombination property of the system. We define the recombination probability for the

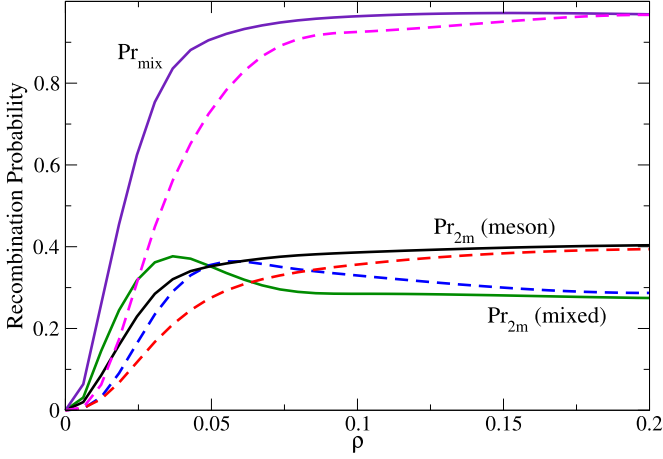


FIG. 11: Recombination probability as a function of the density. The probability for only two mesons recombination (Pr_{2m}) is exhibited for the two mesons and mixed cases (see inner labels). The probability when tetraquarks are accounted as a recombination stage (Pr_{mix}) corresponds to the mixed case. The solid and dashed lines are for ud and ub systems respectively.

two mesons case by:

$$Pr_{2m} = \frac{N(V_{m1} \leftrightarrow V_{m2})}{N(V_{m1}) + N(V_{m2})} \quad (36)$$

where $N(V_i \rightarrow V_j)$ denotes the number of flippings from the i to the j configuration, and $N(V_i)$ is the number of times the system visits the i configuration. If we consider the tetraquark configuration as another possible configuration contributing to the recombination, the probability becomes:

$$Pr_{mix} = [N(V_{m1} \leftrightarrow V_{m2}) + N(V_{m1} \leftrightarrow V_{4Q}) + N(V_{m2} \leftrightarrow V_{4Q}) + N(V_{4Q} \rightarrow V_{4Q})] / [N(V_{m1}) + N(V_{m2}) + N(V_{4Q})] \quad (37)$$

In Figure 11, we show the probabilities as a function of the density. The probability for only two mesons recombination (Pr_{2m}) is exhibited for the two mesons and mixed cases (see inner labels). The probability when tetraquarks are accounted as a recombination stage (Pr_{mix}) corresponds to the mixed case. The solid and dashed lines are for ud and ub systems respectively.

A qualitative estimate of this effect can be exhibited considering a simple expansion model, such that we can evolve the system along the density profile. We can define the color strength function by:

$$\Omega(x) \equiv P_{frag}(t)Pr(x) \quad (38)$$

where $P_{frag}(t) = \exp(-t^2/\tau_{frag}^2)$ is the probability that the system has not yet fragmented, with $\tau_{frag} \approx 3r_h$ the

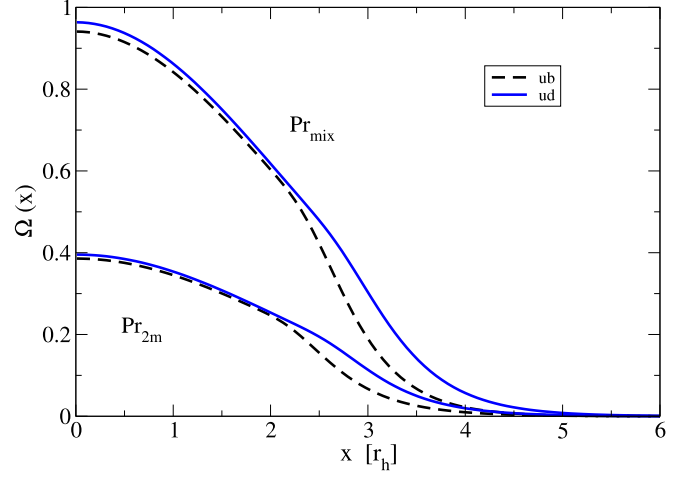


FIG. 12: Color strength due to the recombination probability in the two mesons and mixed cases as a function of the radial size of the system (in units of the meson radius). The solid and dashed lines are for ud and ub systems respectively.

proper lifetime, taken as three times the meson radius r_h [19]. The recombination probability $Pr(\rho)$ can be set in terms of the radius of the sphere (x) corresponding to the given density $\rho = 3N/4\pi r_h^3 x^3$. In Figure 12, we plot the evolution of the color strength as a function of the radial size of the system, in units of the meson radius. The case when considering the tetraquark and meson recombination (Pr_{mix}) largely modifies the estimate when the tetraquark state is not included (Pr_{2m}). The flavor composition modifies the behavior at intermediate distances, and the total effect becomes negligible after four times the hadron radius, corresponding to nearly the size of the end of the overlap of two hadrons.

E. Tetraquark potential

The tetraquark potential depends on the quarks positions and two auxiliary vectors, placed in such away that the total length linking the quarks is the shortest one. These auxiliary vectors are modified in a non-trivial way whenever a single quark changes its position. An effective behavior of the potential can be set as linear respect to the invariant length, $R \equiv \sqrt{\sum r_{ij}^2}$:

$$V(R) = R_0 + BR \quad (39)$$

where R_0 is the value of the potential at zero distance, which is expected to be modified by the short distance coulomb-like correction [27]. In Figure 13, we show the slope B of the linear behavior from the simulation as a function of density for the case when only tetraquarks are allowed to form (solid line) and when mesons and

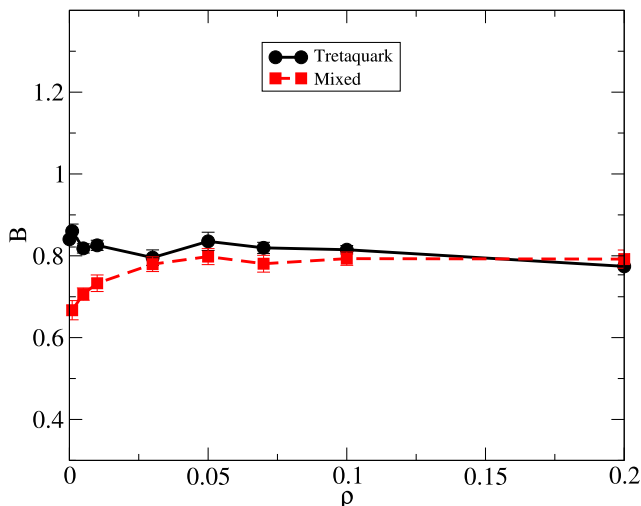


FIG. 13: Slope (B) of the effective tetraquark linear potential as a function of density, for the pure tetraquar system (solid line) and meson- tetraquark mixed system (dashed line).

tetraquarks are allowed to form (dashed line). The slope, in the tetraquark case shows small dependence on the density, and $B(\rho \approx 0) = 0.84 \pm 0.02$. In the mixed case there is a significant density dependence, starting below the corresponding value at zero density ($B(\rho \approx 0) = 0.67 \pm 0.02$) and as the density increases they approach to each other. This behavior is similar when considering different flavor systems.

In Figure 14, we show the effective four-body contact potential, $V_4(\text{contact})$, as a function of density, determined as the average potential irrespective of the length linking the particles. The pure tetraquar system (solid and dashed lines for ub and ud flavors respectively) exhibit a dependence on the mass ratio in the low energy regime and, as density increases, they become similar. The meson-tetraquark mixed system (dotted line) has no dependence on the mass ratio (labeled as mixed), but is very sensitive to the presence of the mesons, becoming very large in the low energy regime. This behavior corresponds to the increasing distance among quarks which are influenced by the two mesons configuration that is trying to bring them apart.

VI. CONCLUSIONS

We have performed a Monte Carlo simulation of two identical light quarks qq and two identical antiquarks $\bar{Q}\bar{Q}$, considering three possible structures: two mesons, tetraquark and mixed configurations. We determined whether it is energetically more favorable to form a tetraquark or two mesons and the mixing among them,

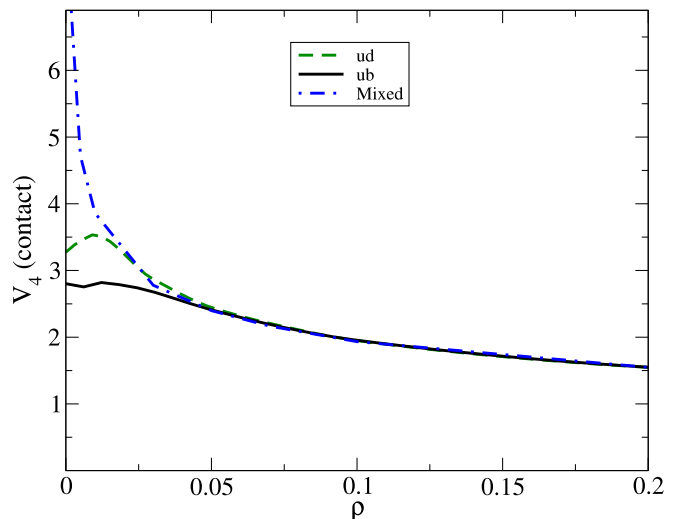


FIG. 14: Effective tetraquark contact potential as a function of density, for the pure tetraquar system (solid and dashed lines for ub and ud flavors respectively) and meson- tetraquark mixed system (dotted line).

as a function of the particle density. Several light-quarks to antiquarks mass ratios were used and exhibited whenever they were found to be relevant. The meson MSR evolution was found to be mass ratio dependent. In fact, the light-light combination (ud) decreases faster than the light-heavy case (ub), while the dependence on being in presence of possible tetraquark configurations is mild. The tetraquark MSR evolution also exhibits a mass ratio dependence, and turns out to be very sensitive to the presence of the mesons.

We have shown that there is a modification in the meson-meson correlation function by the presence of the tetraquark state at intermediate densities, where a bump develops in the near tail of the correlation function, driven by the diquark formation. To gain insight into the features of the tetraquark state, we computed the quark-quark correlation function at several densities. We observed the diquark formation at low densities and the drop on the correlation as the density increased. The quantum correlations among identical particles appeared as Pauli blocking in the short distance regime. In the zero density limit, we determined the correlation functions between quarks and the correlation between a quark and the rest of the particles. A parameterization was found, which is useful to compute additional static properties, in particular we computed the diquark static structure factor, which exhibited a small mass ratio dependence.

We did track the dynamical flipping among configurations and determined the recombination probability evolution as a function of the particle density. We have shown that the probability is largely affected when con-

sidering the tetraquark as an intermediate recombination state. Using a simple model evolution of the system along the density profile we have shown that the recombination effects remain important beyond a half the overlap of two mesons.

The linear behavior of the four-body potential on the invariant length linking the quarks was analyzed and found that the presence of a mixed state is reflected in the decreasing strength of the slope. We determined an effective four-body contact potential as the average strength, irrespective of the length linking the particles. This is very sensitive to the presence of the mesons and when they are not considered there is a dependence on the mass ratio in the low energy regime.

The approach we have followed to the tetraquark system is intended to exhibit the gross features. Certainly, the short distance information and more elaborated interactions should have an effect on the system energy and the corresponding spectrum. In this work, we have limited ourselves to the case of identical quarks and identical antiquarks. Different particles effects should be reflected in the high density regime due to the absence of Fermi correlations.

Appendix: Kinetic term

The kinetic term W Eqn. (29) is evaluated as follows:

Meson: In this case we have two configurations, corresponding to Q_{m_1} and Q_{m_2} . Let us illustrate the form of the contribution from the coordinate x of particle 1, by taking the derivative of the first element of Q_{m_1} :

$$\partial_{x_1} r_{13}^{3/2} = \frac{3}{2} \frac{(x_1 - x_3)}{r_{13}^{1/2}}.$$

Thus, if we compute the contribution for the 3 coordinates and add their squares, we get:

$$[\partial_{x_1} Q_{m_1}]^2 + [\partial_{y_1} Q_{m_1}]^2 + [\partial_{z_1} Q_{m_1}]^2 = \frac{9}{4} r_{13}$$

Analogous results are obtained for the other particles, adding all them up we get:

$$\langle W(Q_{m_1}) \rangle_\lambda = \frac{9\lambda^2}{8} \left(\frac{\langle r_{13} \rangle}{\mu_{13}} + \frac{\langle r_{24} \rangle}{\mu_{24}} \right) \quad (\text{A.1})$$

where μ_{ij} is the corresponding reduced mass. The Q_{m_2} configuration kinetic term is obtained by the $3 \leftrightarrow 4$ exchange.

Tetraquark: In this case we have two additional vectors \vec{k} and \vec{l} , whose explicit dependence on the coordinates of the quarks and antiquarks are unknown. Let us illustrate this implication in the contribution from the coordinate x of particle 1:

$$\begin{aligned} \partial_{x_1} Q_{4Q} &= \partial_{x_1} \left(r_{1k}^{3/2} + r_{2k}^{3/2} + r_{kl}^{3/2} + r_{3l}^{3/2} + r_{4l}^{3/2} \right) \\ &= \frac{3}{2} r_{1k}^{1/2} \partial_{x_1} r_{1k} + \dots \end{aligned} \quad (\text{A.2})$$

The first term derivative can be set as:

$$\begin{aligned} \partial_{x_1} r_{1k} &= [(x_1 - x_k)(1 - \partial_{x_1} x_k) - (y_1 - y_k) \partial_{x_1} y_k \\ &\quad - (z_1 - z_k) \partial_{x_1} z_k] / r_{1k} \end{aligned} \quad (\text{A.3})$$

where we do not know the derivative of the \vec{k} coordinates respect to the x_1 coordinate. The derivatives are numerically evaluated as $\partial_{x_1} x_k \sim \Delta x_k / \Delta x_1$. Analogous terms are evaluated for all the rest of the particles coordinates.

Acknowledgments

We acknowledge the support of DGAPA-PAPIIT UNAM, grant IN106913. We thank Dr. J. Piekarewicz and Dr. A. Ayala for very useful observations.

-
- [1] S. Choi et al. (Belle Collaboration), Phys. Rev. Lett. **100**, 142001 (2008); Z.Q. Liu et al. (Belle Collaboration), Phys. Rev. Lett. **110**, 252002 (2013).
 - [2] M. Ablikim et al. (BES III Collaboration), Phys. Rev. Lett. **110**, 252001 (2013).
 - [3] LHCb Collab. (R. Aaij et al.), Phys. Rev. Lett. **112**, 222002 (2014).
 - [4] R. L. Jaffe, Phys. Rev. D **15** 267(1977).
 - [5] J. Weinstein and N. Isgur Phys. Rev. D **27** 588(1983).
 - [6] N. Isgur and J. Paton Phys. Rev. D **31** 2910(1985).
 - [7] F. Lenz et al., Annals of Phys. **170** 65(1986).
 - [8] J. Carlson and V. R. Pandharipande Phys. Rev. D **43** 1652(1991).
 - [9] D. M. Brink and F. Stancu, Phys. Rev. D **49** 4665(1994).
 - [10] J. Vijande, A. Valcarce, J. M. Richard, Phys. Rev. D **76** 114013 (2007); ibid **87** 034040(2013).
 - [11] Meng-Lin Du, Wei Chen, Xiao-Lin Chen and Shi-Lin Zhu, Phys. Rev. D **87** 014003(2013).
 - [12] Chengrong Deng, Jialun Ping and Fan Wang, Phys. Rev. D **90** 054009 (2014).
 - [13] Pedro Bicudo, Nuno Cardoso, Marco Cardoso. Prog. Part. Nucl. Phys. **67** (2012). 440
 - [14] Eberhard Klempt and Alexander Zaitsev, Phys. Rep. **454** 1(2007).
 - [15] J. Ferretti, G. Galatà and E. Santopinto Phys. Rev. D **90** 054010(2014).
 - [16] A. Esposito et al, Int. Jour. Mod. Phys. A, **30** 1530002(2015).
 - [17] Ping Wang, Stephen R. Cotanch and Ignacio J. General, Eur. Phys. J. C. **55** 409(2008)

- [18] G. Abbiendi et al, (The OPAL Collaboration), Eur. Phys. J. C. **45** 307(2006).
- [19] T. Sjöstrand and V. A. Khoze, Z. Phys.C **62** 281(1994); Phys. Rev. Lett. **72** 28(1994).
- [20] G. S. Bali and K. Schilling, Phys. Rev. D **47** 661(1993).
- [21] J. I. Casaubon and J. P. Cosentino Turk J Phys. **31** 117(2007)
- [22] K. A. Olive et al. (Particle Data Group), Chin. Phys. C **38**, 090001 (2014).
- [23] C. J. Horowitz, E. J. Moniz and John W. Negele, Phys. Rev. D **31** 1689(1985).
- [24] M. Oka and C. J. Horowitz, Phys. Rev. D **31** 2773(1985)
- [25] C. J. Horowitz and J. Piekarewicz Phys. Rev. C **44**, 2753(1991); C. J. Horowitz and J. Piekarewicz Nucl. Phys. A **536** 669(1992); G. Toledo Sánchez and J. Piekarewicz, Phys. Rev. C **65**, 045208 (2002); ibid **70**, 035206 (2004).
- [26] A. Ayala, J. Magnin, L. M. Montano and G. Toledo Sanchez Phys. Rev. C **80** 064905(2009); A. Ayala, M. Martinez, G. Paic and G. Toledo Sanchez, Phys.Rev. C **77** 044901(2008).
- [27] Fumiko Okiharu, Hideo Suganuma and Toru T. Takahashi, Phys. Rev. D **72** 014505(2005).
- [28] A. L. Fetter and J. D. Walecka. *Quantum Theory of Many Particle Systems* (McGraw-Hill, New York, 1971).
- [29] Samuel H. Blitz and Richard F. Lebed, Phys. Rev. D **91** 094025(2015).
- [30] Pedro Bicudo and Marc Wagner, Phys. Rev. D **87**, 114511 (2013).